Draft version February 4, 2025
Typeset using LaTeX **twocolumn** style in AASTeX631

The Mysteries of Be Star: A Comparative Study of the Be Stars Gam Cas and Ksi Per

Yixuan Shao,[1] Xianzhe Tang,[1] and Anthony Lawrenc Chavez[1]

[1] *Department of Physics and Astronomy, Stony Brook University, Stony Brook, NY 11794, USA*

ABSTRACT

This lab report details the observational analysis of the spectra of two Be stars, Gamma Cassiopeiae (Gam Cas) and Xi Persei (Ksi Per). Utilizing data from the BeSS Database, we identified the spectral characteristics of these stars for comparative study. Our observations were conducted at the Mt. Stony Brook Observatory, employing a 14-inch Meade LX200-ACF telescope, a Mesu-200 German Equatorial Mount, and SBIG ST-402 CCD camera and the DADOS Spectrograph. The target Gam Cas (Single Be Star) is located at R.A.$00^h56^m42.5^s$ and Dec.$+60°43'00.3''$, which is in the constellation of Cassiopeia. And the target is 550 ± 10 light-years away with a V magnitude of 2.39, which is a definitely bright star to observe. The target Ksi Per (Double or Multiple Stars) is located at R.A.$03^h58^m57.9^s$ and Dec.$+35°47'27.7''$, which is in the center of the constellation of Perseus. And the target is 1200 light-years away with a V magnitude of 4.06, which is also a definitely bright star to observe. Our observation date is November 2^{nd}, from 6:30pm. to 1:30am.. This report comprehensively presents the findings from our study, highlighting the emission spectrum of Gam Cas and the absorption spectrum of Ksi Per.

1. INTRODUCTION

Be stars, known for their distinctive spectroscopic properties, are fascinating subjects for astronomical research. These stars are characterized by high levels of activity, making them prime candidates for testing and refining theories in stellar physics. Despite significant research efforts, the full understanding of Be stars remains elusive, with many of their features still shrouded in mystery. Their frequent visibility in the night sky has made them popular among both professional astronomers and amateur stargazers. The allure of Be stars is further heightened by their brightness, global visibility, and the rapid evolution of their spectral features, which can range from hours to years.

For effective spectroscopic analysis, selecting a bright target is crucial, especially considering the limitations of observational equipment. Be stars are ideal in this regard, as our targets exhibit high luminosity, facilitating the acquisition of clearer spectra. A unique aspect of Be stars is their occasional "eruptions" during which they expel hydrogen. This phenomenon leads to a notable transformation in their spectroscopic Balmer lines, shifting from absorption to emission. Observing this transition within a single star can be challenging due to limited observation windows. The observed traits of Be stars are currently understood to be a consequence of a gaseous disk surrounding the star, composed of material ejected from it. As Rivinius et al. (2013) introduced in the paper, The phenomena of infrared excess and polarization observed in these stars are attributed to the scattering of the star's light by this disk. Additionally, the emission lines characteristic of Be stars are believed to originate from the reprocessing of the star's ultraviolet light within this gaseous disc.

Initially, our plan was to observe Omi Cassiopeiae (omi Cas), an emission-line star, alongside Xi Persei (ksi Per), known for its absorption features. This would have allowed us to compare the differing Balmer line characteristics between these two types of Be stars. However, due to unforeseen issues with our telescope's guidance system, we had to adjust our target to Gamma Cassiopeiae (Gam Cas) instead of Omi Cas. This change, while unplanned, still aligns with our objective to study and compare the spectral variations between emission and absorption line Be stars, offering valuable insights into their dynamic nature.

In the next section (Target Selection), we provide more detailed parameters and our reasons for choosing these targets. In the section 3 (Observation), we describe the observation-related processes and related information. In section 4 (Data Analysis), we show the processing of the observations and the results obtained, and compare the results with the observations of others in the BeSS database. In the last section (Results), we will display the related result we got from the data and give a possible explanation to its characteristics based on existed Be Star models.

2. TARGET SELECTION

We chose our observational targets from the BeSS database, focusing on stars that were both bright and observable during the late October to November period. The coordinates of our three selected targets, including Omi Cas, are detailed in Table.1. An additional factor in our selection was the proximity of these targets to each other on the celestial chart. This closeness allowed us to use a single bright star situated near them for calibrating our guidance system, thereby streamlining our observation process.

Table 1: A table containing the coordinates for the observation targets.

Object Name	RA	Dec
Ksi Per	3:58	+35:47
Omi Cas	0:44	+48:17
Gam Cas	0:56	+60:43

Fig.1 illustrates that our initial target, Omi Cassiopeiae, reached the ideal observation altitude (above 50°) earlier in the evening. Our alternative target, Gamma Cassiopeiae, displayed a similar observation window to Omi Cas. Subsequently, Xi Persei entered this optimal altitude range, remaining observable until 4 AM. Post 4 AM, moonlight interfered with our ability to continue observations. Throughout our observation period, the altitudes of all targets were consistently above 50 degrees, confirming the feasibility of our observational approach. Additionally, fig.2 presents the trajectory of each target across the sky on the night of observation, indicating their close proximity to each other in the celestial sphere.

3. OBSERVATIONS

We carried out our astronomical observations at the Mt. Stony Brook Observatory using a 14-inch Meade LX200-ACF telescope, complemented by a Mesu-200 German Equatorial Mount, the DADOS Spectrograph and SBIG ST-402 CCD camera. These observations took place on the night of November 2nd, spanning from 6:30 PM to 1:30 AM. Table.2 displays the basic conditions of this observation.

In the initial phase of our observation session, from 6:30 PM to 8:30 PM, we focused on calibration tasks, including adjusting the neon lamp and capturing flat-field images. However, our activities were interrupted by unforeseen challenges: the emergence of clouds and the glare of headlamps from a nearby stadium led us to pause our observations until 9:30 PM.

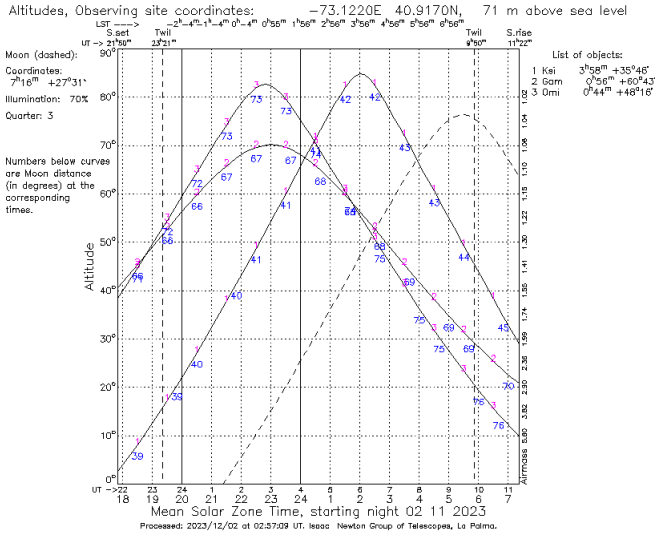

Figure 1: StarAlt Chart for targets Ksi Per, Gam Cas and Omi Cas. Observations lasted for about 7 hours, starting at 6:30pm and ending at 1:30am. The first and last hours were used to perform calibrations with the Neon arclamp and obtain the dark frames.

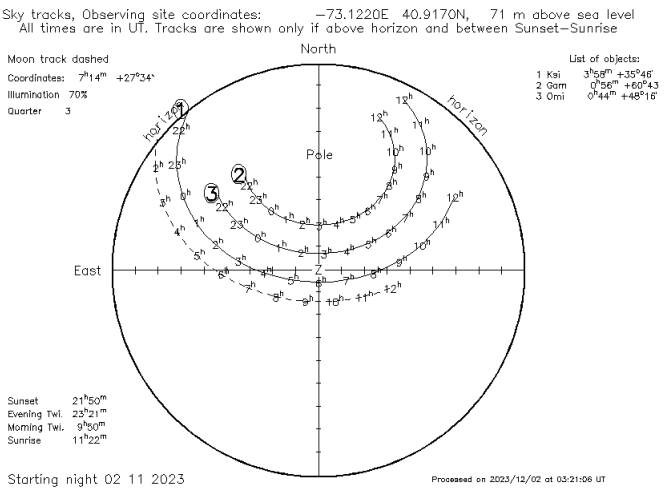

Figure 2: Startrack Chart for targets Ksi Per, Gam Cas and Omi Cas.

Resuming our work, we encountered difficulties in locating Omi Cas, which persisted for approximately an hour and a half. Ultimately, we decided to shift our focus to Gam Cas, our alternate target. For Gam Cas, we successfully captured 10 scientific images, each with an exposure time of 20 seconds. We then turned our attention to Ksi Per, for which we obtained 15 scientific images, this time with a longer exposure duration of 30 seconds each.

Upon completing the observational sequences for both targets, we proceeded to take 10 dark frames for each, using their respective exposure times. This step was crucial for ensuring the quality and accuracy of our final data analysis.

4. DATA ANALYSIS

4.1. *Dark Frame and Flat-Field Calibration*

In our pursuit of enhancing the precision of our observations (Reduce systematical errors), we initially addressed the processing of dark frames, which were specific to each target based on their exposure times: 20 seconds for Gam Cas and 30 seconds for Ksi Per. To create a master dark frame for each target, we computed the median of 10 individual dark frames. This approach helps in effectively reducing noise and correcting for sensor imperfections.

The resulting master dark frame for Gam Cas is presented in fig.3a. This image serves as a crucial reference for identifying and correcting any inherent noise in the images of Gam Cas. Similarly, the master dark frame for Ksi Per is shown in fig.3b. This frame is instrumental in ensuring the accuracy of the observational data for Ksi Per by providing a threshold for hot pixels and then artifact correction.

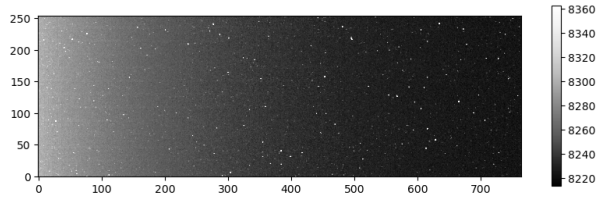

(a) Master Dark frame of Gam Cas

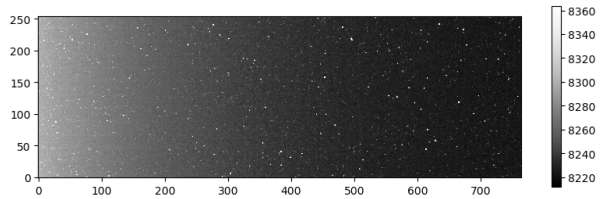

(b) Master dark frame of Ksi Per

Figure 3: Images of the master dark frames for Gam Cas and Ksi Per. The X and Y axis are of the pixel positions in the image, while the colorbar is the value of the pixels in the image.

Following the processing of dark frames, we next focused on the flat-field images, which are crucial for correcting field illumination discrepancies in our observational data. To create a master flat-field image, we calculated the median of 10 individual flat-field images. This technique helps in smoothing out anomalies and ensuring a more uniform response across the field of view.

The master flat-field image derived from this process is showcased in fig.4. In this image, three distinct bands are visible, but for our data analysis, we specifically utilized the second band, which corresponds to the 25 μm slit. As all the scientific images used in our following study were captured within this particular band.

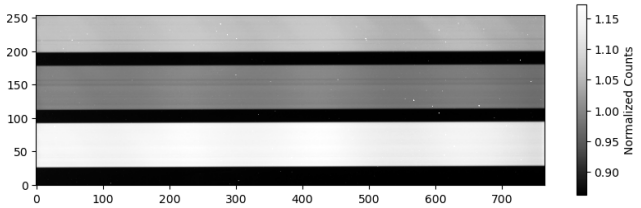

Figure 4: Image of the Normalized Master Flat field. The X and Y axes represent the position of the pixels. For the purposes of data reduction, the middle 25 micron band will be used.

4.2. *Spectroscopic Calibration for Neon Lamp*

Then, using the master dark frame and master flat-field, we could calibrate our Neon Lamp Spectrum to transfer pixels coordinates to wavelength. Since our targets' spectrum range is from 650 nm to 670 nm, we put spectrum line of 633.433 nm at the left side of our camera. Here we use the master dark frame of Ksi Per, since our images for neon lamp have the same exposure time as Ksi Per (30s). Follow the equation:

$$\text{Imagedata} = \frac{\text{Science Image} - \text{Dark frame}}{\text{Flatfield} - \text{Dark Frame}} \quad (1)$$

We get the calibrated spectrum of the Neon Arc lamp (fig.5). Here, we took the median of the neon lamp images for calibration. Based on the standard spectrum

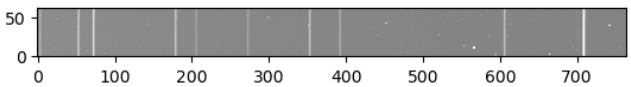

Figure 5: Calibrated spectrum of the Neon Arc Lamp

of Neon Arc Lamp and the x-axis pixel coordinates of the neon spectral lines after calibration, we performed a linear fit to obtain the x-axis pixel coordinates versus

Table 2: Table containing the observation conditions for Nov 2nd. Since both objects were observed within the same night, the conditions experienced little change.

Observing Date	Observatory Name	Weather condition	Illumination	N Exposures	Exposure t (s)	Filter	Autodark
11/2/23	Mt Stony Brook	Partially cloudy	70%	10	20, 30	Visible	OFF

wavelength (fig.7), and its spectrum (fig.6). The best-fit line is:

$$\lambda = (632.805 \pm 0.05) + 0.0989 \times x \quad (2)$$

During our observation, we encountered a technical issue with the DADOS Spectrograph's objective lens, which was not securely fastened at first. This resulted in a slight misalignment after we setup Spectrograph to LX200-ACF Telescope, causing a shift of our coordinates by 1.5 nm to the left side. In subsequent data processing, we preferentially added that offset by default.

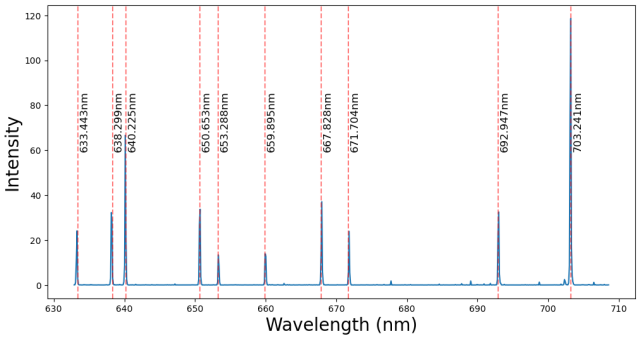

Figure 6: Calibrated Spectrum of the Neon Arclamp matched to the standard wavelength

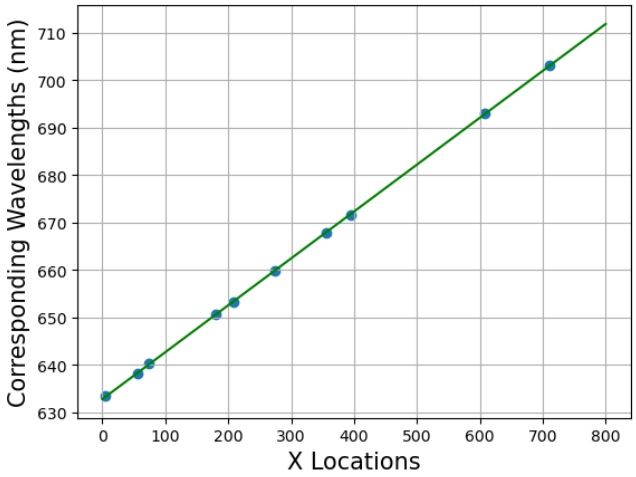

Figure 7: wavelength vs. pixel position linear fit model

4.3. *Calibrated Gam Cas and Ksi Per*

In parallel with our Neon Arclamp calibration, follow the eqa.1, we calibrated both targets to get their calibrated science images. This step was crucial for obtaining calibrated science images, which are essential for detailed analysis.

For Gam Cas, shown in Figure 8a, we selected the best quality science image for our data analysis. Given the relative brightness of Gam Cas, this approach was sufficient to ensure a high-quality analysis. In contrast, our experience with Ksi Per, depicted in fig.8b, was more challenging. Although we captured 15 science images of Ksi Per, only 5 were deemed functional and suitable for analysis. The quality of these images was notably inferior compared to those of Gam Cas. This discrepancy in image quality can be partially attributed to the increasing proximity of the moon to our target during the observation period, which adversely affected the image clarity.

To mitigate these challenges and enhance the quality of our data on Ksi Per, we averaged the best five images. This method allowed us to compensate for the lower quality of individual images and provided a more reliable basis for our subsequent analysis. By averaging, we could reduce noise and improve the overall signal quality, ensuring a more accurate and comprehensive understanding of Ksi Per's spectral characteristics.

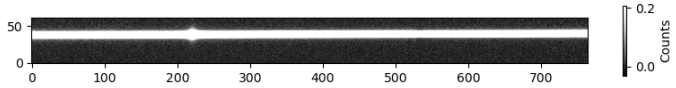

(a) Calibrated Science Image of Gam Cas

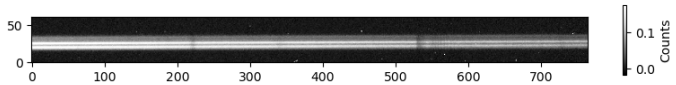

(b) Calibrated Science Image of Ksi Per

Figure 8: Science Images of calibrated Gam Cas and Ksi Per

5. RESUTS

5.1. *Gamma Cassiopeiae*

Once we completed the calibration process and converted the pixel positions into wavelengths, we successfully obtained the spectrum of Gam Cas. As illustrated in Fig.9, it is evident that Gam Cas exhibits a prominent Balmer emission line. This emission line is notably centered around 656.18 ± 0.05 nm, highlighting a significant characteristic of Gam Cas's spectral profile.

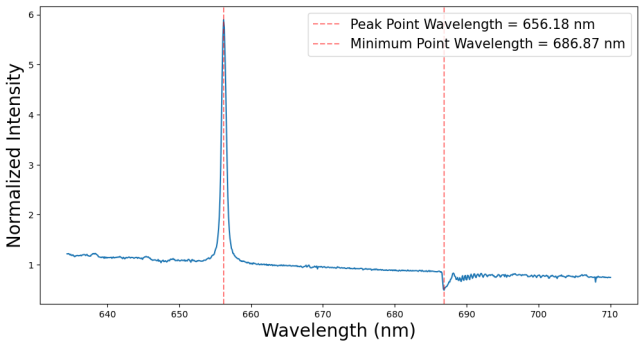

Figure 9: Spectrum of Gam Cas (Wavelength Range from 633 nm to 708 nm)

Upon closely examining the emission line of Gam Cas, particularly focusing on its Balmer emission line, we observed notable variations in its intensity. This observation becomes even more apparent when we compare our current data with previous observations. From the fig.10, it is evident that the intensity of Gam Cas's emission line does not remain constant but varies over the years, indicating dynamic changes in the star's behavior and properties. However, his emission spectral lines have not been significantly shifted(around Hα, wavelength of 656.28 nm in air and 656.46 nm in vacuum). At the same time, its spectral pattern is not significantly altered, from fig.11, we could conclude that we are still observing the pole direction of Gam Cas.

5.2. *Xi Persei*

In contrast to Gam Cas, Ksi Per exhibits absorption lines that, while not as intense, are still markedly noticeable. The spectrum of Ksi Per, as shown in fig.12, spans a wavelength range from 633 to 708 nm. This spectrum is characterized by a discernible decrease trend in intensity compared to that of Gam Cas, indicating a different set of spectral characteristics. The less intense absorption lines of Ksi Per, in comparison to the prominent emission lines of Gam Cas, reflect the distinct astrophysical properties and behaviors of these two stars.

Fig.13 presents our observational data for Ksi Per, particularly focusing on its absorption line. When compared with previous observations, it is noticeable that

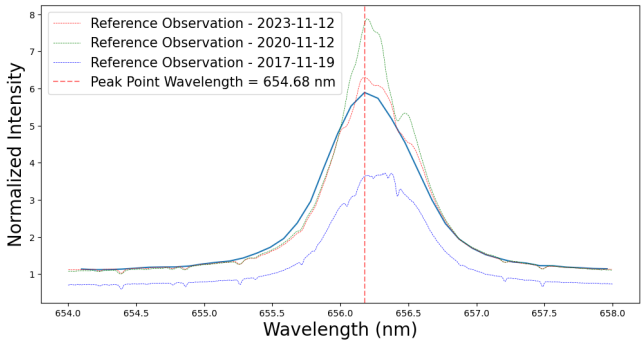

Figure 10: Emission Line in comparison with previous observation in BeSS Database (Wavelength Range: 654-658 nm)

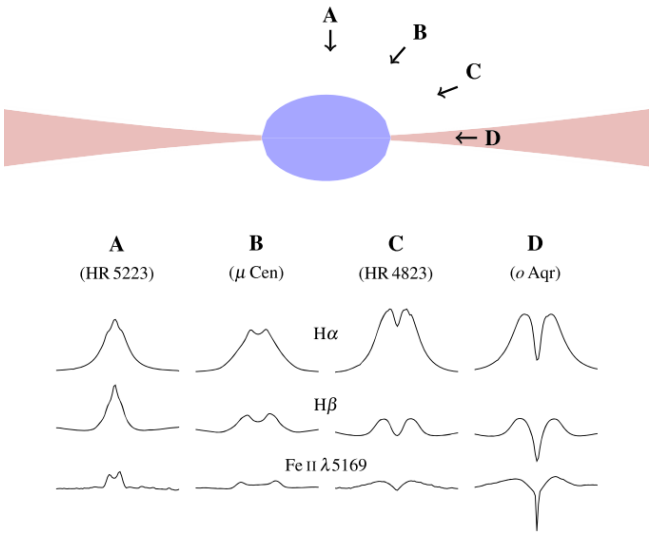

Figure 11: Schematic view of a Be star at critical rotation and with a flared disk. The lower part shows example spectral profiles from pole-on to shell Be star taken from Rivinius et al. (2013), fig.1

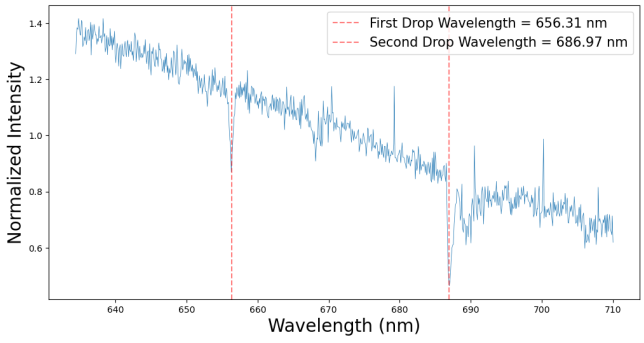

Figure 12: Spectrum of Ksi Per (Wavelength Range from 633 nm to 708 nm)

our data exhibit overall higher intensity levels around

the absorption line. This increased brightness could likely be attributed to the moon's proximity to our target during the observation period, which may have contributed to an overall heightened brightness in our data.

However, due to the lack of spectroscopic data from a stable reference star to calibrate against atmospheric and other background conditions on the day of observation, it remains uncertain whether this increase in intensity is a characteristic inherent to the star itself or a result of the observational environment.

Notably, the position of the absorption line in Ksi Per's spectrum remains consistent, suggesting stability in this aspect. Based on the model of Rivinius et al. (2013), this consistency could indicate that our observations were effectively capturing the star from the direction of its shell disk. The stable position of the absorption line, despite the variations in intensity, provides valuable insight into the orientation and consistency of our observation towards Ksi Per.

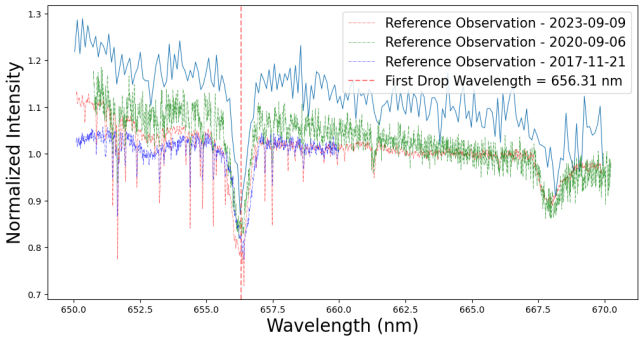

Figure 13: Absorption Line in comparison with previous observation in BeSS Database (Wavelength Range: 650-670 nm)

6. DISCUSSION

When examining the rotational velocities of Gam Cas and Ksi Per, we find that Gam Cas has a rotation speed of $V_{rot} \sin i = 295$ km s^{-1} as reported in Nazé & Motch (2018) (Table 5), while Ksi Per's rotation speed is $V_{rot} \sin i = 220$ km s^{-1} according to Repolust, T. et al. (2004) (Table 1). These values align with the basic model described in Rivinius et al. (2013).

According to the model by Rivinius et al. (2013), the appearance of a Be star's spectrum as either emission or absorption lines can be influenced by the observer's angle. Viewing the star from the poles typically reveals emission lines, whereas observing from the disk's angle tends to show absorption lines. However, when we compare fig.11 with our results for Ksi Per in fig.13, we observe a discrepancy. Based on Rivinius's model, we would expect to see bulges in both segments of the absorption line, which is not evident in our data.

This discrepancy might be explained by the binary system model proposed in El-Badry et al. (2022). According to this model, the interaction within a binary system could account for the variations we observe in the absorption lines of Ksi Per, suggesting that the dynamics of binary systems play a significant role in the spectral characteristics of Be stars. This also somewhat confirms the speculation that Ksi Per may be a binary or multiple star system.

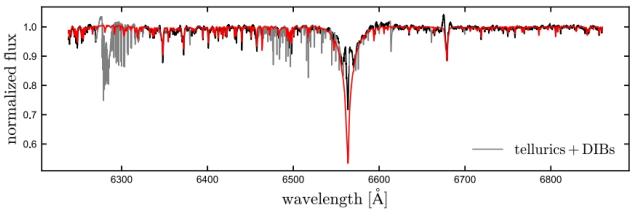

Figure 14: PEPSI spectrum of HD15124 (black) and best-fitting binary model taken from El-Badry et al. (2022), fig.5

An alternative explanation pertains to the presence of a dense circumstellar disk around Be stars. According to the study by Ashraf et al. (2023), the spectral characteristics of a Be star can be significantly influenced by its circumstellar disk. In scenarios where a dense disk is absent, or if the disk's contribution to the observed spectrum is minimal, the star's spectrum will more closely resemble that of a typical B-type star, predominantly displaying absorption lines. These absorption lines arise from the star's atmosphere, where specific wavelengths of light are absorbed by various atmospheric elements.

The presence of a dense circumstellar disk around Ksi Per remains a subject of inquiry, and specific data or detailed studies directly addressing this aspect are not readily available within the scope of this paper. Research into the circumstellar environments of Be stars like Ksi Per is a complex and evolving field, and definitive conclusions about the characteristics of Ksi Per's disk may require more specialized studies or observational data that are beyond the current focus of our research.

7. CONCLUSION

In conclusion, our study of Gamma Cassiopeiae (Gam Cas) and Xi Persei (Ksi Per) has provided valuable insights into the spectral characteristics and behaviors of Be stars. Our observations, conducted at the Mt. Stony Brook Observatory, utilized advanced equipment including a 14-inch Meade LX200-ACF telescope, SBIG ST-402 CCD Camera and the DADOS Spectrograph, en-

abling us to capture detailed spectra of these intriguing stars.

For Gam Cas, we observed a significant Balmer emission line, indicative of its status as a classical Be star with a potentially dense circumstellar disk. The emission line, centered around 656.18 ± 0.05 nm, highlighted the dynamic nature of this star. Our analysis also revealed variations in the intensity of this emission line over time, suggesting changes in the star's circumstellar environment.

In contrast, Ksi Per presented a different scenario. While we successfully captured its spectrum, the intensity of its absorption lines was notably less pronounced compared to Gam Cas. This difference could be attributed to several factors, including the moon's proximity during our observation period, which may have influenced the overall brightness. Our data suggested that Ksi Per might not have a dense circumstellar disk like Gam Cas, or that the disk's orientation relative to our line of sight affected its spectral appearance.

However, our study faced limitations, particularly in confirming the presence of a dense circumstellar disk around Ksi Per. This aspect remains an open question, highlighting the need for further research in this area. Also the resolution of our observations is lower compared to those of others. Perhaps the use of wider and higher definition equipment will help us to draw more conclusions.

Overall, our observations contribute to the broader understanding of Be stars, offering a comparative analysis of two notable examples. The distinct spectral features of Gam Cas and Ksi Per underscore the diverse nature of Be stars and the importance of considering various factors, such as circumstellar disks and observational angles, in their study. This research not only enriches our knowledge of stellar astrophysics but also opens avenues for future investigations into the complex and dynamic environments of Be stars.

APPENDIX

REFERENCES

Ashraf, M., Jose, J., Herczeg, G., & Fang, M. 2023, Journal of Astrophysics and Astronomy, 44, 67, doi: 10.1007/s12036-023-09951-x

El-Badry, K., Conroy, C., Quataert, E., et al. 2022, MNRAS, 516, 3602, doi: 10.1093/mnras/stac2422

Nazé, Y., & Motch, C. 2018, A&A, 619, A148, doi: 10.1051/0004-6361/201833842

Repolust, T., Puls, J., & Herrero, A. 2004, AA, 415, 349, doi: 10.1051/0004-6361:20034594

Rivinius, T., Carciofi, A. C., & Martayan, C. 2013, The Astronomy and Astrophysics Review, 21, doi: 10.1007/s00159-013-0069-0

All Authors and Affiliations

Yixuan Shao,[1] Xianzhe Tang,[1] and Anthony Lawrenc Chavez[1]

[1] *Department of Physics and Astronomy, Stony Brook University, Stony Brook, NY 11794, USA*